AIMS Biophysics, 4(2): 298-315.
DOI: 10.3934/biophy.2017.2.298
Received: 04 March 2017
Accepted: 13 April 2017
Published: 21 April 2017

http://www.aimspress.com/journal/biophysics

Research article

Re-modeling *Chara* action potential: II. The action potential form under salinity stress

Mary Jane Beilby [1,*] and Sabah Al Khazaaly [2]

[1] School of Physics, University of NSW, Kensington, NSW 2052, Australia
[2] Mathematics and Statistics, Western Sydney University**,** Bankstown, NSW 2200, Australia

*** Correspondence:** Email: m.j.beilby@unsw.edu.au.

Abstract: In part I we established Thiel-Beilby model of the *Chara* action potential (AP). In part II the AP is investigated in detail at the time of saline stress. Even very short exposure of salt-sensitive *Chara* cells to artificial pond water with 50 mM NaCl (Saline APW) modified the AP threshold and drastically altered the AP form. Detailed modeling of 14 saline APs from 3 cells established that both the Ca^{2+} pump and the Ca^{2+} channels on internal stores seem to be affected, with the changes sometimes cancelling and sometimes re-enforcing each other, leading to APs with long durations and very complex forms. The exposure to salinity offers further insights into AP mechanism and suggests future experiments. The prolonged APs lead to greater loss of chloride and potassium ions, compounding the effects of saline stress.

Keywords: action potential; Thiel-Beilby model; *Chara*; salinity stress; cytoplasmic Ca^{2+} concentration; Ca^{2+} channels on internal stores; inositol triphosphate; Ca^{2+}-activated Cl^- channels; Ca^{2+} pump

1. Introduction

Thiel and his group measured the rise of Ca^{2+} in *Chara* cytoplasm (and resulting Cl^- channel activation) in response to threshold depolarization of the membrane potential difference (PD) [1,2,3]. They modified animal cell model describing formation of second messenger Inositol 1,4,5-

triphosphate (IP_3) [4,5], which activates Ca^{2+} channels on internal stores [6]. In our first paper [7] we set up PD rate of change equation, where the transient Ca^{2+} concentration increase activated Cl^- channels and the action potential (AP) form was calculated by numerical integration. To improve the fit of the model to AP data, we introduced prompt Ca^{2+} transient across plasma membrane. Sharp, positive-going PD spikes at the beginning of the AP data supported this modification. The feature was particularly visible in cells under saline stress, where the APs were spontaneous [7]. The modeling was initially inspired by observation of these prolonged APs in saline stressed cells. We were able to increase the model AP duration by decreasing the values of coefficients in the Hill equation, describing the Ca^{2+} pumps on internal stores (see Figure 6a in [7]). The present paper provides detailed modeling of saline APs, finding that the form is quite variable: "many-or-none" rather than "all-or-none". To fit such diversity in form, some of the Ca^{2+} channel rate constants also needed modification at the time of saline stress. Different initial IP_3 concentrations were explored. As in the first paper [7] the model suggests range of experiments, as well as prompting a discussion how to distinguish AP from other transients. The effect of spontaneous prolonged APs on the cell under salinity stress is discussed.

2. Materials and Methods

2.1. Materials

As described in paper 1 [7] salt-sensitive *Chara australis* cells survive longer in salinity experiments, if pre-conditioned to osmotic stress in sorbitol artificial pond water (APW: NaCl 1 mM, KCl 0.1 mM, $CaCl_2$ 0.1 mM, neutral pH; with added 90 mM sorbitol) for at least 1hr before exposure to Saline APW (KCl 0.1 mM, $CaCl_2$ 0.1 mM, neutral pH, 50 mM NaCl). The spontaneous APs with prolonged durations were only observed in the Saline APW. The APs were selected from the whole PD record (data-logged at 0.1 s and stored as text files) and input into Mathematica 10 programs. The evolution of the saline AP form was documented in three cells, numbered in order of the modeling process: Cell 1 (4 APs, AP1 shown in Figure 5 of paper 1 [7]), Cell 2 (5 APs, four APs are shown in Figure 6b of paper 1 [7]) and Cell 3 (5 APs, AP5 from Cell 3 is shown in Figure 6a of paper 1 [7]). The fit parameters for all the APs are shown in Tables 1–3.

2.2. Modeling the saline AP form

The derivation of the Thiel-Beilby model is described in detail in paper 1 [7]. This model was used to simulate all the saline APs. The parameters are listed in Tables 1–3. The programs containing the fitted APs can be found on MJ Beilby website link "Action Potential models": http://newt.phys.unsw.edu.au/~mjb/APproj.html. The standard "AP_{av}" modeled to AP data obtained from cells in APW [7] was used to contrast the changes to AP form under salinity stress (see Figure 3, Figure 4 and Tables 1–3).

Table 1a. Cell 1 fit parameters.

Parameter	$AP_{av,\ hyper}$	AP1 (20 s)	AP2 (34 min)	AP3 (90 min)	AP4 (140 min)
ν_r	0.185				
γ_0	0.1 s^{-1}				
γ_1	20.5 s^{-1}				
$p_{1'}$	8.5 μM s^{-1}	8.89 μM s^{-1} 9.3 red 11.1 blue 13.9 green	8.63 μM s^{-1}	8.89 μM s^{-1}	7.8 μM s^{-1}
$p_{2'}$	0.035 μM	0.027 μM 0.027 red 0.025 blue 0.024 green	0.017 μM	0.007 μM	0.007 μM
C_0	1.56 μM				
k_1	12.0 (μM $s)^{-1}$				
k_{-1}	8.0 s^{-1}				
k_2'	15.0 (μM $s)^{-1}$				
k_{-2}	1.65 s^{-1}				
k_3'	1.8 (μM $s)^{-1}$	1.38(μM $s)^{-1}$ 1.41 red 0.8 blue 0.8 green	1.38(μM $s)^{-1}$	1.98 (μM $s)^{-1}$	1.98(μM $s)^{-1}$
k_{-3}	0.04 s^{-1}	0.64 s^{-1} 0.635 red 0.47 blue 0.7 green	0.655 s^{-1}	0.935 s^{-1}	0.95 s^{-1}
IP_3	2.5 μM	0.389 μM 0.49 red 1.0 blue 2.5 green	0.389 μM	0.389 μM	0.389 μM
k_a	2 s^{-1}				
k_i	2 s^{-1}				
ΔCa^{2+} (period of application)	0.0355 (0.04–0.16 s)	0.023 (0.04–0.16 s)	0.04 (0.02–0.16 s)	0.035 (0.04–0.19 s)	0.035 (0.04–0.19 s)

The initial resting PD, RPD, for each cell was adjusted in the model to fit the experimental data. If the RPD was more negative than –100 mV, the appropriate level was obtained by manipulating the proton pump parameters and consequently the I_p/V characteristics (see Figure 1 in paper 1 [7]). At –100 mV the background current, I_{bkg}, dominated the resting membrane characteristics until the outward rectifier current, I_{orc}, became important above ~ –30 mV. Cells exposed to Saline APW for longer times depolarized to PDs above –100 mV and exhibited I/V characteristics that could be modeled by growing contribution from OH^- channels [8,9]. In this case, the amplitude of OH^-

current, I_{OH}, was adjusted to match the cell RPD (Figure 1). The I_{OH} was simulated by the Goldmann-Hodgkin-Katz (GHK) equation, multiplied by the Boltzmann distribution of open probabilities, P_{o-} and P_{o+}, to make the PD-dependence stronger [10,11]. For mathematical details see equations 13, 14a, b in paper 1 [7]. The background and reasoning for modelling of I_{OH} can be found in Beilby and Casanova [12].

Table 1b. Parameters for the membrane transporters.

Parameter	**$AP_{av,hyper}$**	**AP1 (20 s)**	**AP2 (34 min)**	**AP3 (90 min)**	**AP4 (140 min)**
κ_{oi}	140 s^{-1}	140 s^{-1}	102 s^{-1}	65 s^{-1}	40 s^{-1}
k_{io}^0	7000 s^{-1}	7000 s^{-1}	6000 s^{-1}	6000 s^{-1}	6000 s^{-1}
k_{oi}^0	0.1 s^{-1}				
κ_{io}	0.1 s^{-1}				
G_{bkg}	0.5 S m^{-2}	0.5 S m^{-2}	1.5 S m^{-2}	1.5 S m^{-2}	1.5 S m^{-2}
V_{50+}	100 mV				
z_g	1.0				
N_KP_K	6.5 × 10^{-7} m^3 s^{-1}				
$[K^+]_{cyt}$	100 mM				
$[K^+]_o$	0.1 mM				
$[Cl^-]_{cyt}$	10 mM	50 mM			
$[Cl^-]_o$	1.3 mM	50 mM			
$[Ca^{2+}]_{cyt}$	0.02 μM				
$[Ca^{2+}]_o$	0.1 mM				
$G_{Cl,max}$	10 S m^{-2}	40 S m^{-2} 40 red 43 blue 43 green	32 S m^{-2}	25.5 S m^{-2}	19.5 S m^{-2}

Table 2a. Cell 2 fit parameters.

Parameter	**$AP_{av,}$**	**AP1 (142 min)**	**AP2 (160 min)**	**AP3 (168 min)**	**AP4 (245 min)**	**AP5 (268 min)**
ν_r	0.185					
γ_0	0.1 s^{-1}					
γ_1	20.5 s^{-1}					
$p_{1'}$	8.5 μM s^{-1}	8.4 μM s^{-1}	6.8 μM s^{-1}	6.8 μM s^{-1}	6.8 μM s^{-1}	4.8 μM s^{-1}
$p_{2'}$	0.035 μM	0.018 μM	0.02 μM	0.015 μM	0.018 μM	0.02 μM
C_0	1.56 μM					
k_1	12.0					
	$(\mu M\ s)^{-1}$					
k_{-1}	8.0 s^{-1}					
k_2'	15.0					
	$(\mu M\ s)^{-1}$					
k_{-2}	1.65 s^{-1}					
k_3'	1.8 $(\mu M\ s)^{-1}$	1.5 $(\mu M\ s)^{-1}$	0.9 $(\mu M\ s)^{-1}$	0.55 $(\mu M\ s)^{-1}$	0.3 $(\mu M\ s)^{-1}$	0.9 $(\mu M\ s)^{-1}$
k_{-3}	0.04 s^{-1}	0.55 s^{-1}	0.21 s^{-1}	0.21 s^{-1}	0.24 s^{-1}	0.1 s^{-1}
IP_3	2.5 μM	0.5 μM	0.35 μM	0.35 μM	0.35 μM	0.3 μM
k_a	2 s^{-1}					
k_i	2 s^{-1}					
ΔCa^{2+} (period of application)	0.0355 (0.04–0.16 s)	0.015 (0.04–0.16 s)	0.025 (0.04–0.18 s)	0.025 (0.04–0.18 s)	0.025 (0.04–0.18 s)	0.015 (0.04–0.14 s)

The cytoplasmic Cl^- concentration was increased to 50 mM in Saline APW to preserve the AP peak level (see Figure 3). The initial IP_3 concentration, I_0 (see equation 2 in paper 1 [7]), did interact with the other parameters, affecting the AP form in a subtle manner (Figure 2a). The goodness of the model fit was judged by eye, aided by computation of the area difference: area under the data AP—the area under the simulated AP (Figure 2b).

The prompt Ca^{2+} inflow across plasma membrane, $I_{TRP,Ca}$, was simulated as in paper 1 [7]. The data-logging speed in the experiments was too slow to reveal detailed shape of the PD spike (see Figure 3 and Figure 4), so square current pulse was used and the fraction of Ca^{2+} reaching the channels on the stores was adjusted to fit the depolarizing phase of the AP.

Table 2b. Parameters for the membrane transporters.

Parameter	AP_{av}	AP1 (142 min)	AP2 (160 min)	AP3 (168 min)	AP4 (245 min)	AP5 (268 min)
κ_{oi}	140 s^{-1}	I_{OH} $N_{OH}P_{OH}$: 9×10^{-4} m^3 s^{-1}	I_{OH} $N_{OH}P_{OH}$: 1×10^{-4} m^3 s^{-1}	I_{OH} $N_{OH}P_{OH}$: 1×10^{-4} m^3 s^{-1}	I_{OH} $N_{OH}P_{OH}$: 2×10^{-4} m^3 s^{-1}	I_{OH} $N_{OH}P_{OH}$: 2×10^{-4} m^3 s^{-1}
k_{io}^0	7000 s^{-1}	z_{g+}: 1 z_g–: 0.6	z_{g+}: 1 z_g–: 0.6	z_{g+}: 1 z_g–: 0.6	z_{g+}: 1 z_g–: 0.6	z_{g+}: 1 z_g–: 0.6
k_{oi}^0	0.1 s^{-1}	V_{50+}: 350 $V_{50–}$:– 170 mV	V_{50+}: 350 $V_{50–}$: –170 mV	V_{50+}: 350 $V_{50–}$: –170 mV	V_{50+}: 350 $V_{50–}$: –170 mV	V_{50+}: 350 $V_{50–}$: –170 mV
κ_{io}	0.1 s^{-1}					
G_{bkg}	0.5 S m^{-2}	1.8 S m^{-2}	1.8 S m^{-2}	1.8 S m^{-2}	1.8 S m^{-2}	1.8 S m^{-2}
V_{50+}	100 mV					
z_g	1.0					
N_KP_K	6.5×10^{-7} m^3 s^{-1}					
$[K^+]_{cyt}$	100 mM					
$[K^+]_o$	0.1 mM					
$[Cl^-]_{cyt}$	10 mM	50 mM				
$[Cl^-]_o$	1.3 mM	50 mM				
$[Ca^{2+}]_{cyt}$	0.02 μM					
$[Ca^{2+}]_o$	0.1 mM					
$G_{Cl,max}$	10 S m^{-2}	20 S m^{-2}	21 S m^{-2}	20 S m^{-2}	16 S m^{-2}	16 S m^{-2}

3. Results

3.1. AP evolution with time in Saline APW

Cell 1 AP1 demonstrated how fast the AP form responded to exposure to Saline APW. After only 20 s, with the RPD still very negative at –235 mV, the AP duration had more than doubled (Figure 3a, see also Figure 5a in paper 1 [7]). However, the repolarizing stage followed similar trend

to AP_{av} (included in Figure 3a in blue). This gradual repolarization presented first modeling challenge, as changing the Hill coefficients, p_1' and p_2', in the Ca^{2+} pump model alone did not provide the right shape. The rate constants k_3' and k_{-3}, controlling the backward and forward transition between the activated Ca^{2+} channel state and final inactivated Ca^{2+} channel state (see equation 1 in paper 1 [7]), had to be modified to achieve reasonable fit (Table 1a, Figure 3b). AP2 (34 min of saline exposure) looked very similar to AP1, but the duration was slightly longer and the repolarization stage slightly shorter (see Table 4 for summary of AP data and Figure 3a). AP3 (90 min saline exposure) form had changed further: there was a distinct overshoot bulge at the beginning of the AP, reminiscent of the peak of AP_{av}, and the repolarization stage was more abrupt, giving the AP square appearance. AP4 (140 min saline exposure) was similar in initial stages, but had much longer duration of almost 6 s and repolarized even more abruptly (Figure 3a, Table 4). The membrane RPD has depolarized for the last two APs to –175 and –155 mV, respectively (Table 4). Figure 3b shows that modeled APs, superimposed on the data as yellow lines, provide satisfactory fit, describing the main features of each AP.

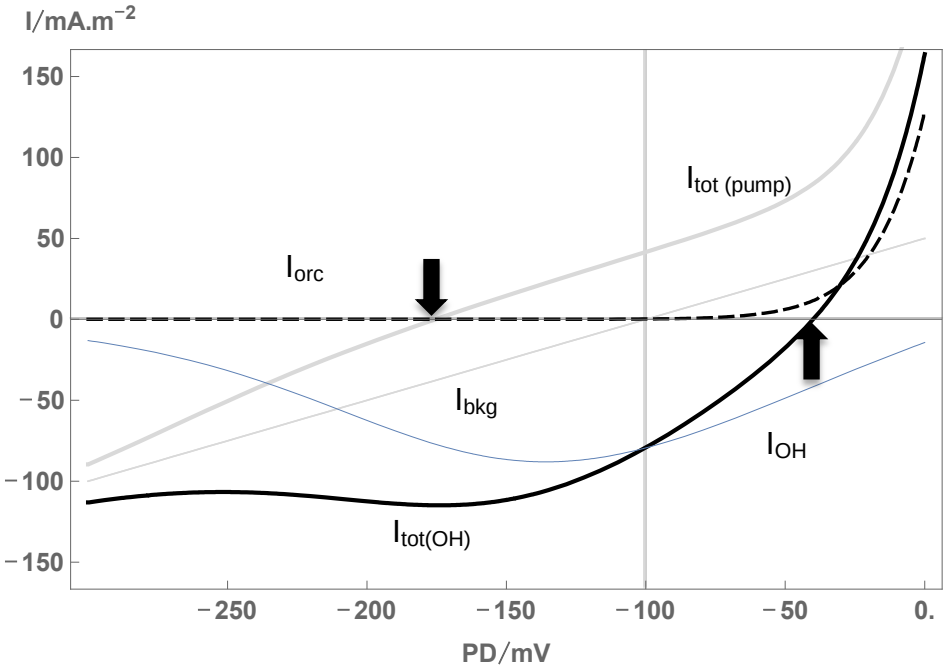

Figure 1. I/V characteristics of the most conductive transporters in *Chara* plasma membrane after long exposure to Saline APW: the OH^- channels become the dominant feature of the membrane conductance: I_{OH}, (thin curved line), the background current, I_{bkg}, (thin straight line), the outward rectifier, I_{orc}, (long-dashed line) and the total current $I_{tot(OH)}$ (thick black line). The values of the model parameters were selected to match the RPD (see upward arrow) of the depolarized cells. The pump dominated I/V characteristics, $I_{tot(pump),}$ used in calculation of AP_{av} [7] are included for comparison and shown as thick gray line. Note the difference of RPD in pump dominated state (downward arrow) and OH^- channel dominated state (upward arrow).

a

b

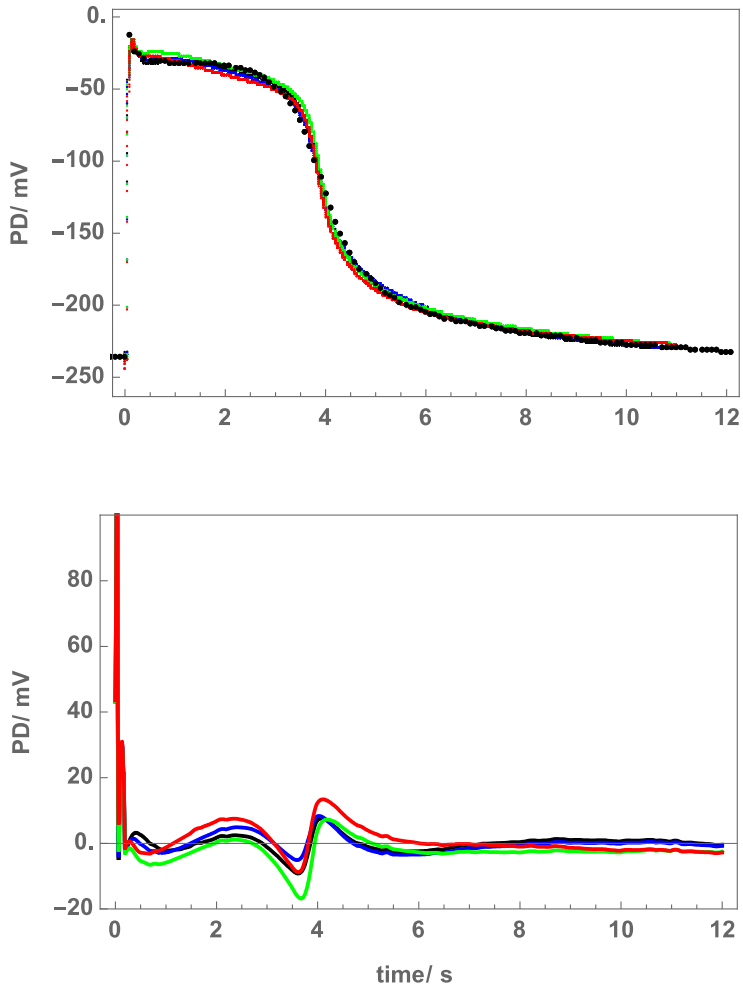

Figure 2. The effect of initial IP_3 concentration I_0. Data fitted (points) come from Cell 1, AP1, exposure to Saline APW of 20s. (a) AP model with I_0 concentrations in μM: 0.389 (black), 0.49 (red), 1.0 (blue), 2.5 (green). For the values of the other model parameters, see Table 1, AP 1. (b) The goodness of fit judged by the area difference (area under data AP—area under model AP).

The initial IP_3 concentration, I_0 (see equation 2 in paper 1 [7]) subtly influenced the AP form (Figure 2a). The best fit of the model for Cell 1 was found with I_0 = 0.389 μM. The small changes in AP form for other concentrations are shown with different colors, the quality of the fit is expressed as area difference (see Methods, Figure 2b). Changing I_0 required adjustment in p_1', p_2', k_3', k_{-3} and $G_{Cl,max}$ parameters for the best fit (Table 1). Such parameter interaction increased complexity of the fitting process.

The Cell 1 data suggest that the duration of AP may increase with saline exposure. Following the evolution of Cell 2 dispels that hypothesis: the durations of the five APs seem to vary at random, with the last AP5 being the second shortest (Figure 4, Table 4). Similarly in Cell 3 AP1 is much longer than AP2 (Figure 5). However, the repolarization once again became faster with longer saline exposures in both Cell 2 and Cell 3 APs (Figure 4, Table 4).

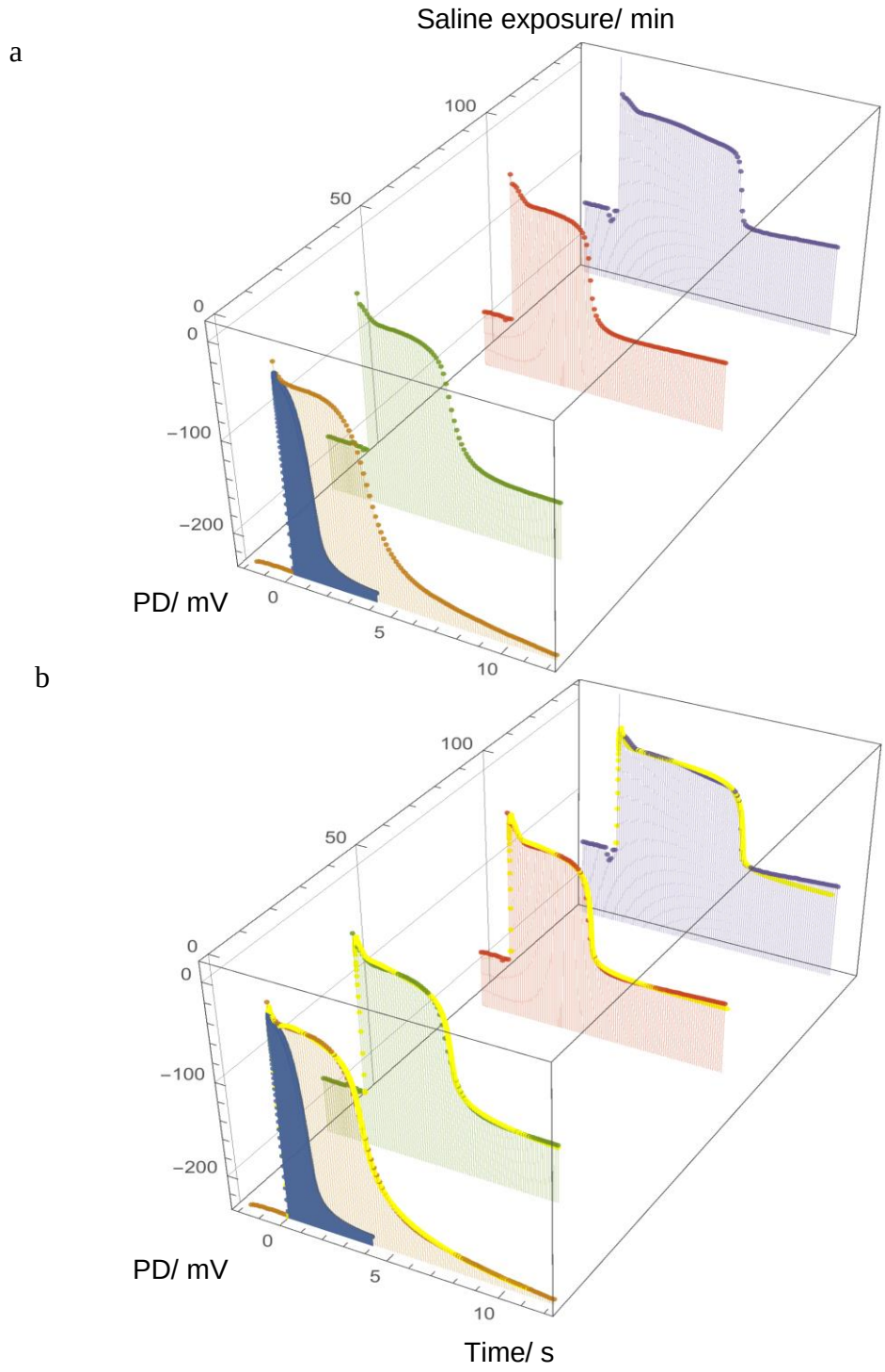

Figure 3. Evolution of the AP form as function of exposure to Saline APW in Cell 1. (a) The spontaneous APs were recorded at 20 s, 34 min, 90 min and 140 min after the cell was challenged with Saline APW. The AP_{av}, fitted to cells in APW (dark blue profile), was included for comparison. As Cell 1 was quite hyperpolarized in Sorbitol APW, before exposure to saline, AP_{av} was adjusted through the pump model parameters (see $AP_{av,hyper}$ in [7] and parameter values in Table 1). (b) The modeled APs were superimposed on the data as yellow lines, showing good correspondence (parameters in Table 1). Note the more gradual re-polarization phase in the early exposure APs.

3.2. Refractory period

Cell 3 provided another insight. Apart from AP2, all other APs displayed long durations (Table 4, Figure 6). AP1 and AP5 both featured secondary peaks towards the end of the transient (Figure 6a, Figure 6b). The refractory period of *Chara* AP under normal conditions was found to be between 6 and 60 s [14]. Shepherd et al. 2008 [15] observed spontaneous repetitive APs in 100 mM NaCl/0.1 mM $CaCl_2$ medium of 30 s duration and between 26 and 37 s apart. Consequently the secondary peaks in present data were treated as re-excitation and smaller amount of IP_3 was introduced into the model. While the simulation produced secondary peaks, detailed fit was difficult (Table 3, Figure 6).

Table 3a. Cell 3 parameters.

Parameter	**AP_{av}**	**AP1 (1 min)**	**AP2 (18 min)**	**AP3 (82 min)**	**AP4 (84 min)**	**AP5 (115 min)**
ν_r	0.185					
γ_0	0.1 s^{-1}					
γ_1	20.5 s^{-1}					
$p_{1'}$	8.5 μM s^{-1}	1.65 μM s^{-1}	10.5 μM s^{-1}	2.1 μM s^{-1}	2.8 μM s^{-1}	0.651 μM s^{-1}
$p_{2'}$	0.035 μM	0.029 μM	0.045 μM	0.045 μM	0.045 μM	0.027 μM
C_0	1.56 μM					
k_1	12.0 $(\mu M\ s)^{-1}$					
k_{-1}	8.0 s^{-1}					
k_2'	15.0 $(\mu M\ s)^{-1}$					
k_{-2}	1.65 s^{-1}					
k_3'	1.8 $(\mu M\ s)^{-1}$	1.72 $(\mu M\ s)^{-1}$	0.1 $(\mu M\ s)^{-1}$	1.7 $(\mu M\ s)^{-1}$	1.7 $(\mu M\ s)^{-1}$	1.72 $(\mu M\ s)^{-1}$
k_{-3}	0.04 s^{-1}	0.054 s^{-1}	1.4 s^{-1}	0.6 s^{-1}	0.6 s^{-1}	0.695 s^{-1}
IP_3	2.5 μM	2.5 μM	0.23 μM	2.5 μM	2.5 μM	2.5 μM
k_a	2 s^{-1}					
k_i	2 s^{-1}					
ΔCa^{2+} (period of application)	0.0355 (0.04–0.16 s)	0.02 (0.04–0.16 s)	0.021 (0.04–0.18 s)	0.02 (0.04–0.18 s)	0.02 (0.04–0.18 s)	0.02 (0.04–0.18 s)

AP1 Extra bump: Ip_0 = 0.15 μM, turned on at 18.5 s.

AP5 Extra bump: Ip_0 = 0.0065 μM, turned on at 53.05 s.

Table 3b. Parameters for the membrane transporters.

Parameter	**AP_{av} hyper**	**AP1 (1 min)**	**AP2 (18 min)**	**AP3 (82 min)**	**AP4 (84 min)**	**AP5 (115 min)**
κ_{oi}	140 s^{-1}	120 s^{-1}	70 s^{-1}	$I_{OH:}$ $N_{OH}P_{OH:}$ 10×10^{-4} m^3 s^{-1}	$I_{OH:}$ $N_{OH}P_{OH:}$ 10×10^{-4} m^3 s^{-1}	50 s^{-1}
k_{io}^0	7000 s^{-1}	6000 s^{-1}		z_{g+}: 1 z_{g-}: 0.6	z_{g+}: 1 z_{g-}: 0.6	6000 s^{-1}
k_{oi}^0	0.1 s^{-1}			V_{50+}: 350 V_{50-}: –170 mV	V_{50+}: 350 V_{50-}: –170 mV	
κ_{io}	0.1 s^{-1}					
G_{bkg}	0.5 S m^{-2}	1.2 S m^{-2}	1.5 S m^{-2}	1.8 S m^{-2}	1.8 S m^{-2}	1.6 S m^{-2}
V_{50+}	100 mV					
z_g	1.0					
N_KP_K	6.5 × 10^{-7} m^3 s^{-1}					
$[K^+]_{cyt}$	100 mM					
$[K^+]_o$	0.1 mM					
$[Cl^-]_{cyt}$	10 mM	50 mM				
$[Cl^-]_o$	1.3 mM	50 mM				
$[Ca^{2+}]_{cyt}$	0.02 μM					
$[Ca^{2+}]_o$	0.1 mM					
$G_{Cl,max}$	10 S m^{-2}	27 S m^{-2}	13 S m^{-2}	70 S m^{-2}	70 S m^{-2}	13.5 S m^{-2}

3.3. Statistical summary

The data were collected from 14 spontaneous APs coming from 3 cells. The exposures to saline stress varied between 0.3 and 268 min, with RPDs ranging from –235 to –74 mV. The repolarization times mostly decreased for all cells as function of the saline exposure time. The initial spikes, thought to be due to prompt Ca^{2+} transient across plasma membrane, exhibited varying shapes and amplitudes. Some of the variation arises from insufficient data-logging speed (see methods). The maximal PDs of the measured spikes varied from –28 to +58 mV (Figure 3, Figure 4, Table 4). Some cells exhibited multiple spikes (Cell 2: APs 2, 3 and 4). The flat prolonged peaks of the APs were

often not horizontal, so we defined maxima and minima for each AP (Table 4). The average level section of the AP varied between –29 and –39 mV (Table 4). The duration varied between 2.5 and 50 s, with average of 12.8 ± 4.1 s (Table 4). However, even the shortest saline APs had longer durations than AP_{av}.

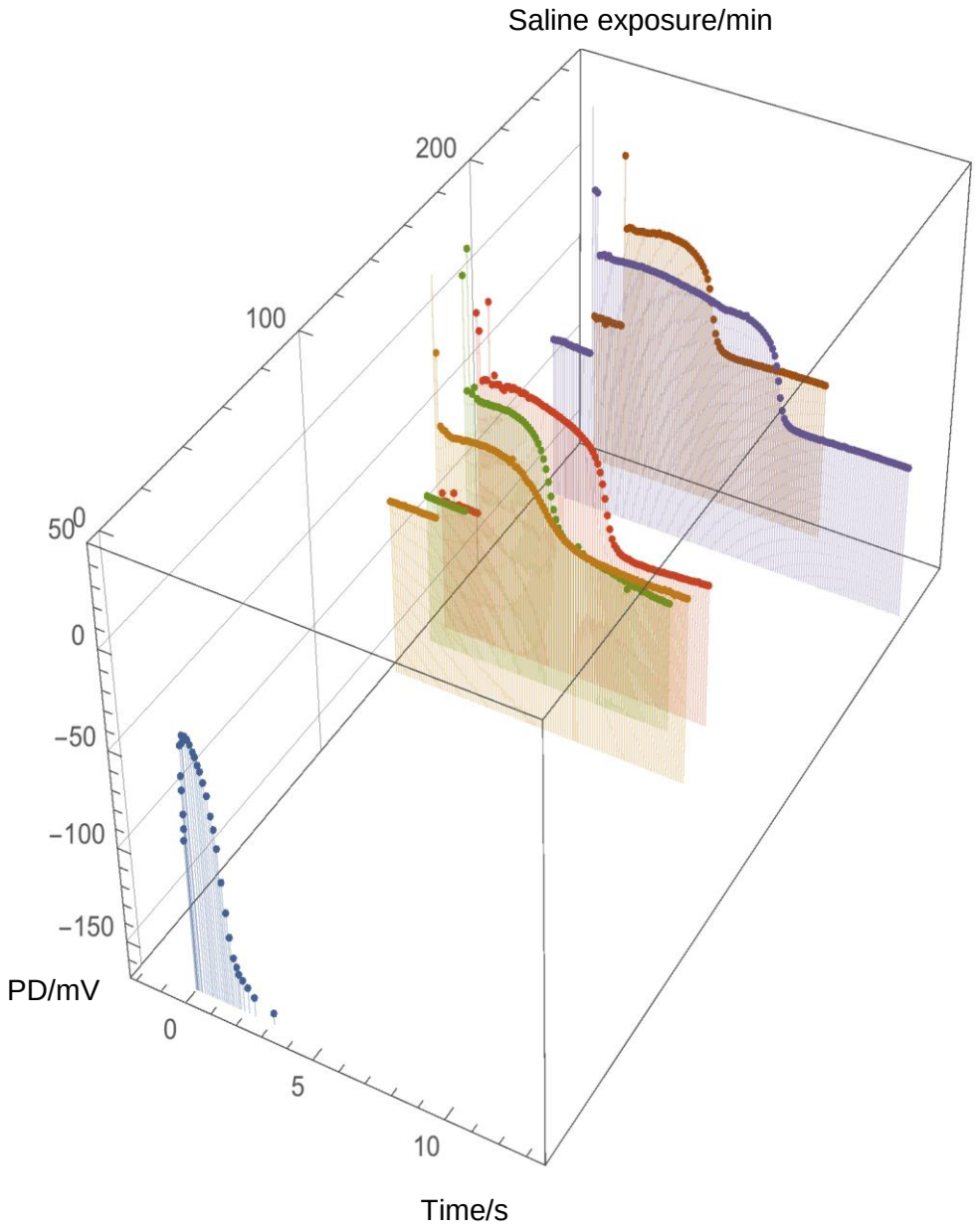

Figure 4 Evolution of the AP form as function of exposure to Saline APW in Cell 2. AP_{av} is included at the beginning of the series: AP1 (142 min saline exposure), AP2 (160 min saline exposure), AP3 (168 min saline exposure), AP4 (245 min saline exposure) and AP5 (268 min saline exposure). Note the changes in duration, with AP5 being the second shortest AP from the series despite very long saline exposure. Note also the multiple initial spikes in APs 2, 3 and 4.

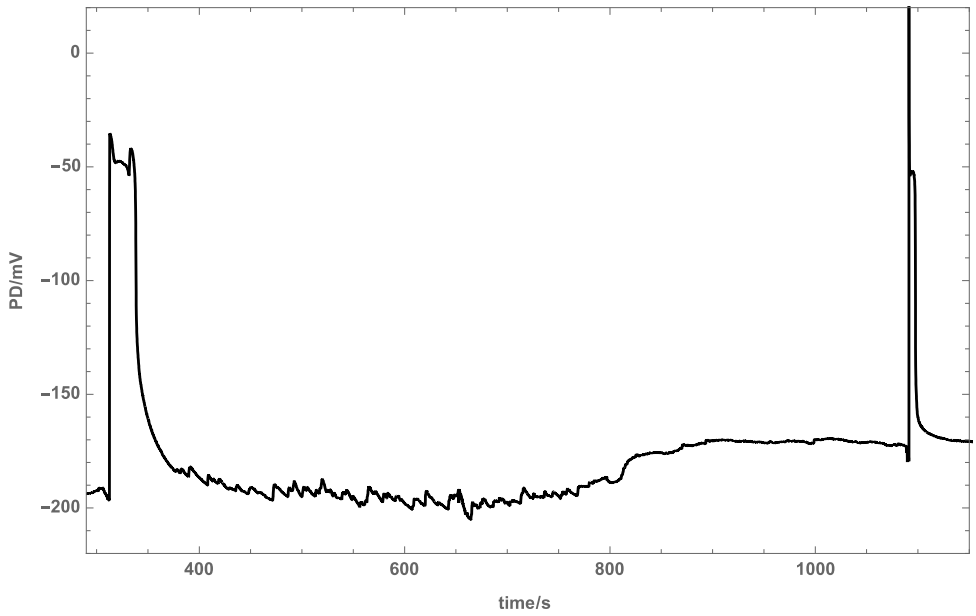

Figure 5. Cell 3: AP1 and AP2 display great variation in form and duration, although AP2 fired at 18 min of saline exposure, while AP1 exposure was only 1 min. Note typical saline noise at the end of AP1 lasting until 800 s of the experiment [13]. Note also the unusual shape of AP1. The time axis shows time from the exposure to Saline APW.

Table 4. Summary of AP parameters.

Saline Exposures/ min	cell 1: 0.3, 34, 90, 140
	cell 2: 142, 160, 168, 245, 268
	cell 3: 1, 18, 82, 84, 115
RPD/mV	cell 1: –235, –178, –175, –155
	cell 2: –74, –88, –97, –81, – 87
	cell 3: –196, –177, –90, –75, –167
Repolarization time/s	cell 1: 8, 3.8, 2.2, 1
	cell 2: 2.9, 2.8, 1.9, 1.4, 1.2
	cell 3: 45, 3.2, 12, 10, 10, 2.9
Spike peak/mV (multiple peaks in brackets)	cell 1: –11, –12, –13, +46
	cell 2: +51, (+34, +48), (+8, +16), +57, +6
	cell 3: –28, +10, +16, –6, +51
AP peak/mV Average: –38.9 ± 3.8 –29.0 ± 3.8	cell 1: –31 to –34, –38 to –48, –40 to –48, –35 to –52
	cell 2: –27 to –36, –26 to –35, –23 to –38, –24 to –38, –29 to –35
	cell 3: –46 to –52, –52 to –58, –2 to –11, –1 to –11, –32 to –48
Duration/s Average: 12.8 ± 4.1	cell 1: 2.5, 3.2, 3.1, 5.7
	cell 2: 3.7, 2.9, 4.4, 7.3, 3.2
	cell 3: 19 + 6 (secondary peak), 5.8, 33, 30, 50

a

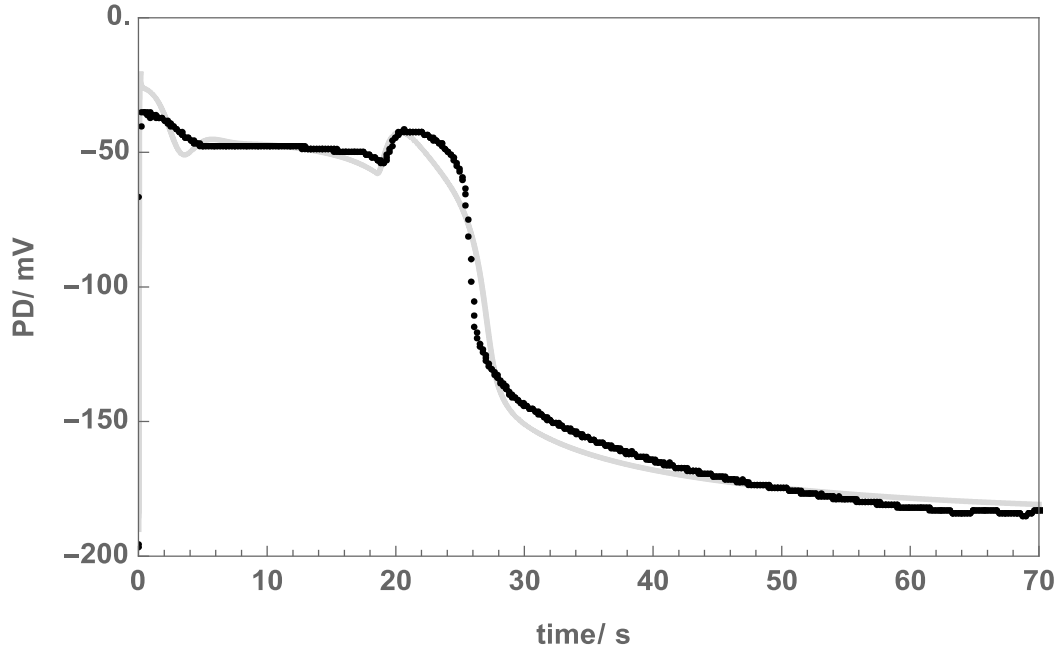

b

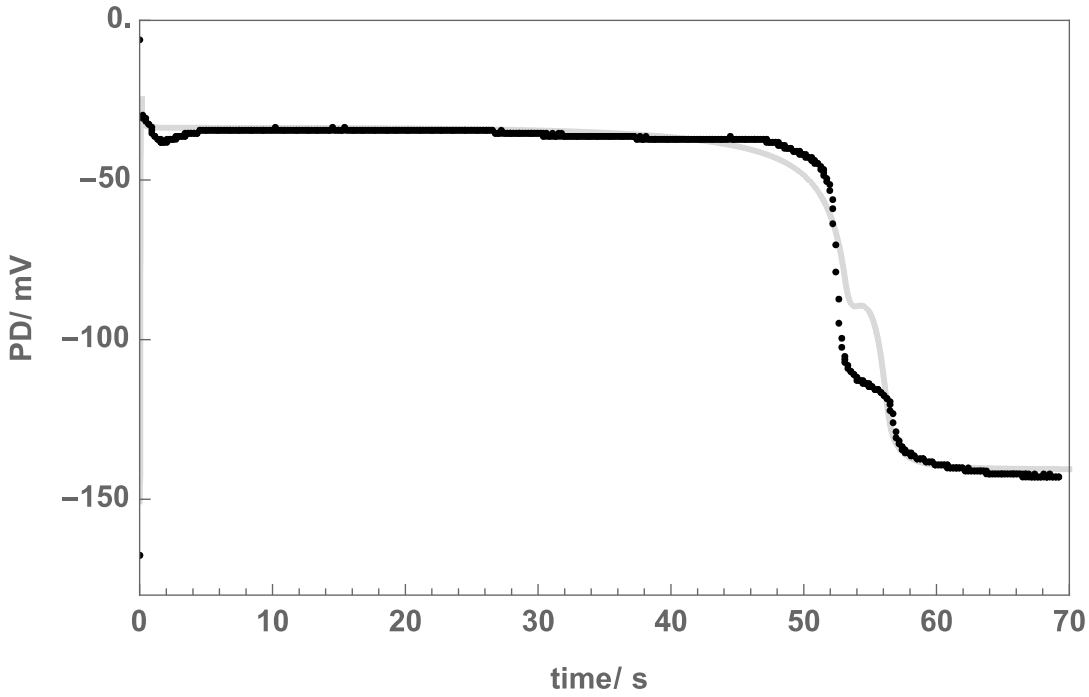

Figure 6. (a) AP1 (1 min of saline exposure) and (b) AP5 (115 min saline exposure) of Cell 3 depolarized the membrane for comparatively long periods of 20 and 50 s. Note secondary peaks at about 20 s in (a) and 50 s in (b). These features were simulated by sudden increase in IP_3 (Table 3) but were difficult to fit closely (light gray lines). AP5 is one of the longest *Chara* APs observed so far under saline stress.

4. Discussion

4.1. Can AP be distinguished from other transients?

Under salinity stress, the APs in salt-sensitive *Chara australis* become "many-or-none", rather than "all-or-none" transient. The diversity involves bulges (e. g. Cell 1: APs 2–4) or dips (e.g. Cell 2: APs 1, 2 and 5, Cell 3: AP5) after the initial prompt spike. The flat part of the AP can slope in hyperpolarizing (Cell 1 APs) or depolarizing (Cell 2: AP 1 and 5) direction. Not only there is a diversity of form, but also the APs at similar saline exposures sometime display large differences (e. g. the two APs in Figure 5). This behavior could only be simulated with the model parameters p_1', p_2', k_3' and k_{-3} varying in almost random fashion (Tables 1–3). These parameters control the Ca^{2+} inflow into cytoplasm from the stores and pumping Ca^{2+} back into the stores. Plots of the parameters as function of saline exposure time display a lot of scatter (see supplementary Figure 1 on http://newt.phys.unsw.edu.au/~mjb/APproj.html). However, p_1'and p_2' mostly decreased with saline exposure time (with exception of Cell 3 p_2' at 18, 82 and 84 min saline exposure), while k_3' seemed initially unaffected (with exception of Cell 3 at 18 min saline exposure) and decreased at longer exposures, and k_{-3} increased and then decreased at similar exposures. Clearly more data are needed for conclusive analysis, especially with Cell 3 exhibiting very long APs, which required different combination of parameter values.

Considering the diversity in form, can we be sure that these saline transients are in fact APs? Firstly, we can see the transition from AP_{av} after short exposures to Saline APW (Figure 3a, also Figure 5a in paper 1 [7]). Most saline APs start with the positive going spike of putative Ca^{2+} inflow across plasma membrane. Further, due to cytoplasmic Ca^{2+} rise, the characean AP is coupled to sudden stoppage of cytoplasmic streaming, which takes ~5 min to recover [16]. This effect was always noted at the time of the experiments. The AP peak, or the plateau in long APs, was found between –30 and –40 mV similar to AP_{av}. Finally, the Thiel-Beilby model can accommodate the main features of the diverse saline AP form. Thus we feel fairly confident, that the saline APs are produced by the same mechanisms as AP_{av}, but with some of it's many processes affected by salinity. Could we simulate the diverse saline AP form by another model? The alternative scenario is the inflow of Ca^{2+} from the outside through plasma membrane voltage-dependent channels. The prolonged Ca^{2+} inflow from the outside under saline stress would probably lead to greater depolarization of the AP peak than observed experimentally, but voltage clamp experiments might be necessary to investigate this possibility.

Interestingly, the shape of the saline AP with the initial spike, the long plateau and the rapid recovery are reminiscent of cardio myocyte AP [17]. While the underlying channels in the myocyte AP are different (fast Na^+ channel for the initial spike and two types of K^+ channel for repolarization), there is also Ca^{2+} inflow, followed by more Ca^{2+} input from internal stores. In both systems the high internal Ca^{2+} transforms the electrical impulse into mechanical contraction of the heart muscle or the "green muscle" of the cytoplasmic streaming stoppage.

While the re-excitation at the end of AP1 and AP5 of Cell 3 is plausible, as the refractory periods of those durations have been observed [14,15], there is also possibility of superposition of the saline noise [13]. This is more likely in AP1 (Figure 5), where the noise is visible at the end of

excitation. However, the secondary bulge is similar to that at the beginning of the AP (Figure 6a) and unlike the spiky saline noise [13]. Alternatively, the long depolarization might produce small amounts of IP_3, which would be normally insufficient to start an AP, but as there is still lot of Ca^{2+} in the cytoplasm, more Ca^{2+} channels are activated.

4.2. The effect of prolonged APs on the salinity stressed cell

Shepherd et al. [15] compared the effects of 100 mM NaCl with either 1.0 mM or 0.1 mM $CaCl_2$, noting that low external Ca^{2+} caused depolarization to PDs above the AP threshold and spontaneous repetitive prolonged APs, which usually lead to cell death. In our experiments with Saline APW of 50 mM NaCl/0.1 mM $CaCl_2$, spontaneous APs at shorter intervals also seemed to speed up the cell collapse with RPD close to zero and permanent cytoplasmic streaming cessation (e.g. Cell 2).

Under normal circumstances, the APs signal mechanical deformation or injury to the cell and cessation of cytoplasmic streaming allows the wound healing process to start [18]. So, why is AP so damaging to the cell under salinity stress? The plateau in the saline AP between –30 and –40 mV activates the outward rectifier current (Figure 1) and cell loses K^+ (and Cl^- through Ca^{2+}-activated Cl^- channels) in each AP. With the pump getting gradually inactivated and the RPD depolarizing close to and eventually above –100 mV, the loss of K^+ becomes irreversible. In a healthy cell, K^+ is one of the most abundant inorganic cations, which activate enzymes, stabilize protein synthesis and contribute to cell turgor [19]. Under salinity stress Na^+ enters the cytoplasm through the voltage-independent non-selective channels, that conduct the background current [15], and competes for K^+ binding sites, being similar in physicochemical structure. However, the similarity is not close enough for Na^+ to perform the same functions and K^+-dependent metabolic processes are inhibited [20]. The mechanisms for salinity effects on the Ca^{2+} channels and pumps on the internal stores are not clear at present. Perhaps K^+ stabilizes the channel and pump proteins and the gradual replacement by Na^+ leads to somewhat random changes in their function. In general, plants need to maintain high cytoplasmic K^+/Na^+ ratio to be salt tolerant [19,20]. Cl^- is regarded as essential micronutrient, important in oxygenic photosynthesis and needed for turgor generation [21]. With the collapse of the proton electrochemical gradient due to salinity activation of H^+/OH^- channels [8], the cell is no longer able to import Cl^- [22] and export Na^+ [23]. Shepherd et al. [15] designated the spontaneous repetitive APs as "point of no return" at the time of saline stress. As Characeae are sister plants to ancestors of land plants [24,25], the lesson of AP contribution to salt stress may be also relevant to agriculturally important plants.

5. Conclusion

The detailed modeling of the *Chara* AP undergoing salinity stress revealed complex and variable form. The main features of the saline APs could be fitted by the Thiel-Beilby model, varying the parameters of the Ca^{2+} pump (Ca^{2+} removal from the cytoplasm), and the activation/inactivation of the Ca^{2+} channels on the inside stores (Ca^{2+} inflow into cytoplasm). The initial activating concentration of IP_3 also influenced the AP form. Experiments to explore saline *Chara* AP:

(1) The excitability of *Chara* cells can be irreversibly abolished by exposure to La^{3+} [26] and the cells can then be tested for longer survival in Saline APW, compared to untreated cells.
(2) The external Ca^{2+} is important in cell survival in saline stress [15]. The saline AP can be explored with different Ca^{2+} content of saline medium. Voltage clamp experiments will resolve whether Ca^{2+} comes from the outside or internal stores.
(3) Is Na^+ the only ion that modifies the AP form? A range of ions similar to Na^+ should be tested.

Acknowledgments

MJB thanks Dr. Vadim Volkov for stimulating discussions at the time of modeling of the saline APs and to referees for constructive comments.

Conflicts of Interest

All authors declare no conflicts of interest in this paper.

References

1. Biskup B, Gradmann D, Thiel G (1999) Calcium release from $InsP_3$-sensitive internal stores initiates action potential in *Chara*. *FEBS Let* 453: 72–76.
2. Wacke M, Thiel G (2001) Electrically triggered all-or-none Ca^{2+} liberation during action potential in the giant alga *Chara*. *J Gen Physiol* 118: 11–21.
3. Wacke M, Thiel G, Hutt MT (2003) Ca^{2+} dynamics during membrane excitation of green alga *Chara*: model simulations and experimental data. *J Memb Biol* 191: 179–192.
4. Thiel G, MacRobbie EAC, Hanke DE (1990) Raising the intercellular level of inositol 1,4,5-triphosphate changes plasma membrane ion transport in characean algae. *EMBO J* 9: 1737–1741.
5. Zherelova OM (1989) Activation of chloride channels in the plasmalemma of *Nitella syncarpa* by inositol 1,4,5-trisphosphate. *FEBS Let* 249: 105–107.
6. Othmer HG (1997) Signal transduction and second messenger systems, In: Othmer HG, Adler FR, Lewis MA, Dallon J, Editors, *Case studies in Mathematical Modeling—Ecology, Physiology and Cell Biology*, Prentice Hall, Englewood Cliffs, NJ.
7. Beilby MJ, Al Khazaaly S (2016) Re-modeling *Chara* action potential: I. from Thiel model of Ca^{2+} transient to action potential form. *AIMS Biophysics* 3: 431–449.
8. Beilby MJ, Al Khazaaly S (2009) The role of H^+/OH^- channels in salt stress response of *Chara australis*. *J Memb Biol* 230: 21–34.
9. Al Khazaaly S, Beilby MJ (2012) Zinc ions block H^+/OH^- channels in *Chara australis. Plant Cell Environ* 35: 1380–1392.
10. Amtmann A, Sanders D (1999) Mechanisms of Na^+ uptake by plant cells. *Adv Bot Res* 29: 75–112.
11. Beilby MJ, Walker NA (1996) Modelling the current-voltage characteristics of *Chara* membranes. I. the effect of ATP and zero turgor. *J Memb Biol* 149: 89–101.
12. Beilby MJ, Casanova MT (2013) *The Physiology of Characean Cells.* Berlin, Springer.

13. Al Khazaaly S, Walker NA, Beilby MJ, et al. (2009) Membrane potential fluctuations in *Chara australis:* a characteristic signature of high external sodium. *Eur Biophys J* 39: 167–174.
14. Beilby MJ (1976) An investigation into the electrochemical properties of cell membranes during excitation, School of Physics, University of New South Wales, Sydney, Australia, Doctor of Philosophy thesis.
15. Shepherd VA, Beilby MJ, Al Khazaaly S, et al. (2008) Mechano-perception in *Chara* cells: the influence of salinity and calcium on touch-activated receptor potentials, action potentials and ion transport. *Plant Cell Environ* 31: 1575–1591.
16. Williamson RE, Ashley CC (1982) Free Ca^{2+} and cytoplasmic streaming in the alga *Chara*. *Nature* 296: 647–651.
17. Jaye DA, Xiao YF, Sigg DC (2010) Basic Cardiac Electrophysiology: Excitable Membranes, In: Sigg DC, Iaizzo PA, Xiao YF, He B, *Cardiac Electrophysiology Methods and Models*, Springer.
18. Shimmen T (2001) Involvement of receptor potentials and action potentials in mechano-perception in plants. *Aust J Plant Physiol* 28: 567–576.
19. Sharma T, Dreyer I, Riedelsberger J (2013) The role of K^+ channels in uptake and redistribution of potassium in model plant *Arabidopsis thaliana. Front Plant Sci* 4: 224.
20. Maathuis FJ, Amtmann A (1999) K^+ nutrition and Na^+ toxicity: The basis of cellular K^+/Na^+ ratios. *Annals of Botany* 84: 123–133.
21. Raven JA (2017) Chloride: essential micronutrient and multifunctional beneficial ion. *J Exp Bot*: 68: 359–367.
22. Beilby MJ, Walker NAW (1981) Chloride transport in *Chara*. I. Kinetics and current voltage curves for probable proton symport. *J Exp Bot* 136: 42–54.
23. Munns R, Tester M (2008) Mechanisms of salt tolerance. *Annu Rev Plant Biol* 59: 651–681.
24. Wodniok S, Brinkmann H, Glockner G, et al. (2011) Origin of land plants: do conjugating green algae hold the key? *BMC Evol Biol* 11: 104–114.
25. Timme RE, Bachvaroff TR, Delwiche CHF (2012) Broad phylogenomic sampling and the sister lineage of land plants. *PLoS One* 7: e29696.
26. Beilby MJ (1984) Current-voltage characteristics of the proton pump at *Chara* plasmalemma: I. pH dependence. *J Membrane Biol* 81: 113–125.

AIMS Press